# Molecular evolution of oxygenated organic molecules in a cloud-influenced forested mountain environment

Yi Zhang[1,2], Wei Zhou[1,2], Weiqi Xu[1,2], Yan Li[1,2], Yu Zhang[1,2], Zijun Zhang[1,2], Bojiang Su[3], Ning Zhang[4], Eleonora Aruffo[5], Junfeng Wang[4], Piero Di Carlo[6], Lanzhong Liu[7], Xiaole Pan[1,2], Zifa Wang[1,2], Douglas R. Worsnop[8], Yele Sun[1,2]

[1]State Key Laboratory of Atmospheric Environment and Extreme Meteorology, Institute of Atmospheric Physics, Chinese Academy of Sciences, Beijing 100029, China
[2]College of Earth and Planetary Sciences, University of Chinese Academy of Sciences, Beijing 100049, China
[3]State Key Laboratory of Advanced Environmental Technology, Guangzhou Institute of Geochemistry, Guangzhou Institute of Geochemistry, Chinese Academy of Sciences, Guangzhou 510640, China
[4]Nanjing University of Information Science and Technology, Nanjing 210044, China
[5]Department of Science, University "G.d'Annunzio" of Chieti-Pescara, Chieti 66100, Italy
[6]Department of Advanced Technologies in Medicine & Dentistry, University "G. d'Annunzio" of Chieti- Pescara, Chieti 66100, Italy
[7]Shanghuang Atmospheric Boundary Layer and Eco-Environment Observatory, Institute of Atmospheric Physics, Chinese Academy of Sciences, Jinhua 321203, China
[8]Aerodyne Research Inc., Billerica, Massachusetts 01821, United States

*Correspondence to*: Yele Sun (sunyele@mail.iap.ac.cn)

**Abstract.** Atmospheric oxygenated organic molecules (OOMs) link the oxidation of volatile organic compound to secondary organic aerosol formation, yet their molecular evolution in cloud-influenced forested mountain environments remains poorly constrained. Here, gas-phase OOMs were measured using an iodide-adduct chemical ionization mass spectrometer at a high-altitude forested station in southeastern China during autumn 2023. Among the 1503 identified ions, isoprene-derived OOMs were primarily controlled by daytime OH-initiated oxidation, whereas monoterpene-derived OOMs were driven by coupled OH and $NO_3$ chemistry. Positive matrix factorization identified nine atmospherically relevant OOM factors, revealing that biogenic oxidation dominated OOM production during warm periods (mean temperature ~20 °C), accounting for 68–79% of the total OOMs, whereas anthropogenic and regional transport factors became prominent during cooler periods (below 15 °C), accounting for up to 63% of the total budget. Cloud processes exerted a pronounced influence on OOM composition through competitive wet scavenging and multiphase chemistry. During cloud events, isoprene-derived and monoterpene-derived organic nitrates (ISO-ONs and MT-ONs) decreased by 75% and 46%, respectively, while the relative contribution of MT-ONs increased from 23% to 40%, suggesting different responses of ISO-ONs and MT-ONs to cloud processing. Furthermore, the contribution of sulfur-containing OOMs increased substantially, consistent with a contribution from aqueous/multiphase processing. These results demonstrate that cloud processing influences the composition and sources of OOMs in forested mountain atmospheres and should be considered when evaluating the atmospheric fate of biogenic oxidation products.

## 1 Introduction

Biogenic volatile organic compounds (BVOCs), primarily emitted by terrestrial vegetation, constitute the largest sources of reactive carbon in the atmosphere (Guenther et al., 1995). Once released, BVOCs are oxidized by atmospheric oxidants such as hydroxyl radicals (OH·), ozone ($O_3$), and nitrate radicals ($NO_3$·), producing a wide range of oxygenated organic molecules (OOMs). Due to their low volatility and high condensability, OOMs are pivotal drivers of secondary organic aerosol (SOA) formation and new particle formation (NPF) (Hallquist et al., 2009; Ehn et al., 2014; Bianchi et al., 2019). By modulating aerosol mass loading and cloud condensation nuclei (CCN) activity, OOMs significantly influence atmospheric radiative forcing, air quality and regional climate (Sun and Ariya, 2006; Hoyle et al., 2009; Tröstl et al., 2016). Consequently, understanding the molecular composition, formation mechanisms, and atmospheric evolution of OOMs has become a central topic in atmospheric chemistry, particularly BVOC-derived species.

Recent advancements in chemical ionization mass spectrometry (CIMS) have enabled the real-time, molecular-level characterization of atmospheric OOMs. Among these techniques, iodide-adduct CIMS (I-CIMS) has emerged as a robust tool for detecting multifunctional oxygenated organic compounds and organic nitrates (ONs), facilitating extensive investigations into atmospheric oxidation processes (Lee et al., 2014; Lee et al., 2016; Ye et al., 2021; Sun et al., 2025). Previous field campaigns using I-CIMS have revealed substantial variability in OOM composition and formation pathways across diverse environments. While boreal forest OOMs are typically dominated by highly oxygenated monoterpene-derived autoxidation products (Mohr et al., 2019), studies in temperate and tropical forests have highlighted the importance of isoprene oxidation products (Zha et al., 2024), reflecting differences in BVOC emission patterns and oxidation regimes. In contrast, urban observations have further demonstrated the significant contribution of anthropogenic volatile organic compounds (AVOCs) and high-$NO_x$ levels to the formation of oxygenated ONs and other nitrogen-containing OOMs (Li et al., 2026; Zhang et al., 2026c). Recent measurements at high-altitude sites, including the southeastern Tibetan Plateau and the Chacaltaya station in the Bolivian Andes, have shown that OOM composition in mountain environments is influenced by anthropogenic emissions, regional transport, and free-tropospheric air masses (Yu et al., 2025; Zha et al., 2024). Collectively, these studies indicate that the molecular characteristics of OOMs are strongly controlled by the interplay between precursor emissions and local atmospheric oxidation regimes.

Compared to well-studied forest and urban areas, high-altitude mountain sites represent a unique atmospheric environment where local biogenic emissions, regional transport, and free-tropospheric influences frequently interact. In southeastern China, mountain stations are often surrounded by dense subtropical forests and enveloped in clouds due to complex topography and monsoon circulations (Shen et al., 2025; Liu et al., 2025; Ding et al., 2025). Cloud processes can substantially alter the abundance and composition of OOMs through wet scavenging, aqueous-phase oxidation, and gas-particle partitioning (Ervens et al., 2011; McNeill, 2015; Herrmann et al., 2015). Moreover, cloud droplets provide reactive media for multiphase oxidation and can modify the fate of ONs through dissolution and hydrolysis, potentially reshaping the molecular composition of OOMs (Takeuchi and Ng, 2019; Wang et al., 2021). These processes may alter both the volatility distribution and source contributions

of OOMs, ultimately affecting SOA formation and atmospheric oxidative capacity. Despite the growing number of I-CIMS field measurements worldwide, molecular-level observations of OOMs at mountain sites remain limited. In particular, the effects of cloud processing on OOM composition, volatility characteristics, source apportionment, and biogenic ON formation have not been comprehensively investigated.

To address these knowledge gaps, a field campaign was conducted at a high-altitude forested mountain site in southeastern China during autumn 2023. Online measurements of OOMs were performed using an I-CIMS, together with complementary observations of BVOCs, trace gases, meteorological parameters, and aerosol chemical composition. The objectives of this study were to (1) characterize the molecular composition and volatility distribution of OOMs in this unique environment, (2) investigate the oxidation pathways of major biogenic OOMs and ONs, (3) quantify the contributions of different OOM sources and formation processes using positive matrix factorization (PMF), and (4) evaluate how cloud processing affects OOM composition and source profiles. This work provides new insights into the formation and evolution of OOMs in forested mountain environments and enhances our understanding of cloud–aerosol–chemistry interactions.

## 2 Sampling and methods

### 2.1 Sampling site and instruments

The field campaign was conducted at the Shanghuang Eco-Environmental Observatory of the Chinese Academy of Sciences (hereafter, SH; 119.51° E, 28.58° N), located in Jinhua, Zhejiang Province, China, at an elevation of 1128 m above sea level. The site is a representative mountaintop background station in southeastern China. The observation period lasted from 22 September to 21 October 2023. Surrounded by dense forests, the site is strongly influenced by active biogenic emissions (Zhang et al., 2024). In addition, frequent cloud events occurred during the campaign due to the combined effects of the East Asian monsoon climate and mountainous terrain. More detailed descriptions of the site can be found in Wang et al. (2025).

Gaseous OOMs were measured using an I-CIMS (Tofwerk AG, Switzerland). The sampling inlet was located on the rooftop of the third floor of the SH station. Ambient air was drawn through approximately 5 m of perfluoroalkoxy (PFA) Teflon tubing at a total flow rate of 10 L $min^{-1}$, resulting in a residence time of approximately 0.35 s before entering the instrument. Of the flow, ~1.8 L $min^{-1}$ was introduced into the ion–molecule reaction region (IMR) of the I-CIMS. In the IMR, analyte molecules were ionized via adduct formation with iodide reagent ions ($I^-$). The iodide ions were generated by passing high-purity nitrogen over a permeation tube containing methyl iodide ($CH_3I$), which was maintained at approximately 60 °C, and subsequently ionizing the resulting vapor in a soft X-ray ion source (Lee et al., 2014). The reagent ions selectively clustered with oxygenated organic molecules, forming iodide adduct ions that were subsequently transferred into a time-of-flight mass spectrometer (ToF-MS) for mass analysis (Junninen et al., 2010). To ensure data quality, instrument background measurements were performed every 2–3 days throughout the campaign. The I-CIMS operated with a time resolution of 1 s, enabling continuous real-time monitoring of atmospheric OOMs. VOCs were simultaneously measured using a Vocus proton-transfer-reaction time-of-flight

mass spectrometer (Vocus PTR-MS; Tofwerk AG, Switzerland). Instrument operation and data processing followed the same procedures as those applied during the 2022 measurement campaign at the same site (Zhang et al., 2024).

Meteorological parameters, including air temperature and relative humidity (RH), were measured using a standard meteorological probe (HC2S3, Campbell Scientific Inc., USA). Wind speed and wind direction data were obtained from the ERA5 reanalysis dataset (Hersbach et al., 2023). Ambient $O_3$ concentrations were measured using a gas analyzer (Model 49i, Thermo Scientific Inc., USA), while nitrogen dioxide ($NO_2$) concentrations were determined using a thermal dissociation laser-induced fluorescence (TD-LIF) system (Di Carlo et al., 2013). The chemical composition of fine particulate matter ($PM_{2.5}$) was measured using a Time-of-Flight Aerosol Chemical Speciation Monitor (ToF-ACSM; Aerodyne Research Inc., USA). Detailed descriptions of the aerosol chemical composition measurements and data processing procedures can be found in Zhang et al. (2026b). It should be noted that cloud events were automatically identified using a ground-based counterflow virtual impactor (GCVI; Brechtel Manufacturing Inc.) (Shingler et al., 2012). To maintain consistency with previous analyses of cloud processing at the SH site, the cloud-event numbering used in this study follows that reported by Zhang et al. (2026b). A summary of the instruments deployed during the campaign is provided in Table S1.

## 2.2 Data analysis

### 2.2.1 Mass spectra analysis

The data obtained from the I-CIMS and Vocus PTR-MS were processed using the Tofware package (Tofwerk AG, v3.2.5). More than one thousand molecular ions were identified within the mass-to-charge ratio (*m/z*) range of 170–500 Th. These species mainly included oxygenated organic compounds, organic acids, and several inorganic species such as nitryl chloride and dinitrogen pentoxide. Because iodide-adduct chemical ionization exhibits high sensitivity toward multifunctional OOMs with moderate oxidation states and relatively high molecular polarity, while showing lower sensitivity toward weakly oxygenated and extremely highly oxidized species, the present study primarily focuses on OOMs containing more than two oxygen atoms. In particular, CHO and CHON compounds were selected for further analysis owing to their dominant contribution to the detected OOM pool.

A semi-quantitative approach was applied to estimate the mixing ratios of OOMs measured by the I-CIMS (Isaacman-Vanwertz et al., 2018; Ye et al., 2021). Instrument sensitivities were constrained using voltage-scanning experiments to characterize the relative sensitivity of individual OOMs, while the dependence of ion transmission efficiency on analyte mass was parameterized to account for mass-dependent transmission effects. The resulting sensitivity and transmission-efficiency relationships were then applied to convert the measured ion signals into semi-quantitative OOM mixing ratios. The detailed calibration procedures are provided in Text S1. The Vocus PTR-MS was calibrated periodically throughout the campaign using a certified VOC standard gas mixture. The calibration enabled quantitative measurements of BVOCs, including isoprene and monoterpenes, as well as the major isoprene oxidation products methyl vinyl ketone (MVK) and methacrolein (MACR). The

resulting concentration data were subsequently used to investigate precursor–product relationships and oxidation pathways of OOM formation.

### 2.2.2 PMF analysis

PMF analysis was conducted using the PMF Evaluation Tool (PET, v3.08) (Ulbrich et al., 2009). Following screening based on signal-to-noise ratio (S/N), data completeness, and molecular characteristics, a total of 576 OOM species were selected for PMF analysis. Details regarding the PMF data preparation and factor selection procedures are provided in the Text S2. Following the evaluation of factor profiles, diurnal variations, precursor characteristics, and relationships with external tracers, the eleven-factor solution was selected as the most physically meaningful representation of the dataset. Among the resolved factors, nine were interpreted as atmospherically relevant sources or processes and were designated as Daytime ISO oxidation, Forenoon ISO+MT oxidation, Afternoon ISO oxidation, Afternoon ISO+MT oxidation, Nighttime ISO+MT oxidation, Nitrogen-containing species, Sulfur-containing species, Anthropogenic organic nitrates, and Regional transport. The remaining two factors (BG1 and BG2) were dominated by instrumental background signals and did not exhibit meaningful atmospheric characteristics, were therefore not considered in the subsequent analysis.

## 3 Results and discussion

### 3.1 Meteorology and trace gases

Figure 1 presents the diurnal variations of meteorological parameters and trace gases during the observation period. Based on the prevailing meteorology and pollutant concentrations, the campaign was divided into four representative periods: P1 (22-23 September), characterized by cloud influence characterized by cloud influence, relatively strong daytime solar radiation, and RH approaching saturation (99.8%); P2 (27-29 September), a warm and cloud-free period, which recorded the highest average temperature (22.4 °C) and the most intense solar radiation; P3 (5-12 October) , a cold and dim period dominated by persistent precipitation, resulting in the lowest temperature (average: 11.5 °C) and minimal solar radiation; and P4 (16-20 October), a clear-sky period marked by elevated pollution levels with low RH. Affected by wet scavenging during cloud and precipitation events, $PM_{2.5}$ concentrations during P1 and P3 were substantially lower than those during the cloud-free periods (P2 and P4) (6.0 vs. 16.0 μg $m^{-3}$). In addition, $PM_{2.5}$ concentrations during P4 were the highest among all four periods, indicating the most severe pollution conditions during this stage. In contrast, the concentrations of $O_3$ and $NO_2$ began to increase after approximately 16:00 local time and reached maxima around 20:00, creating favourable conditions for nocturnal $NO_3$ radical formation and subsequent nighttime oxidation chemistry. Temporal variations during the observations and more detailed comparisons among the four periods are summarized in Figs. S1-S2 and Table S2.

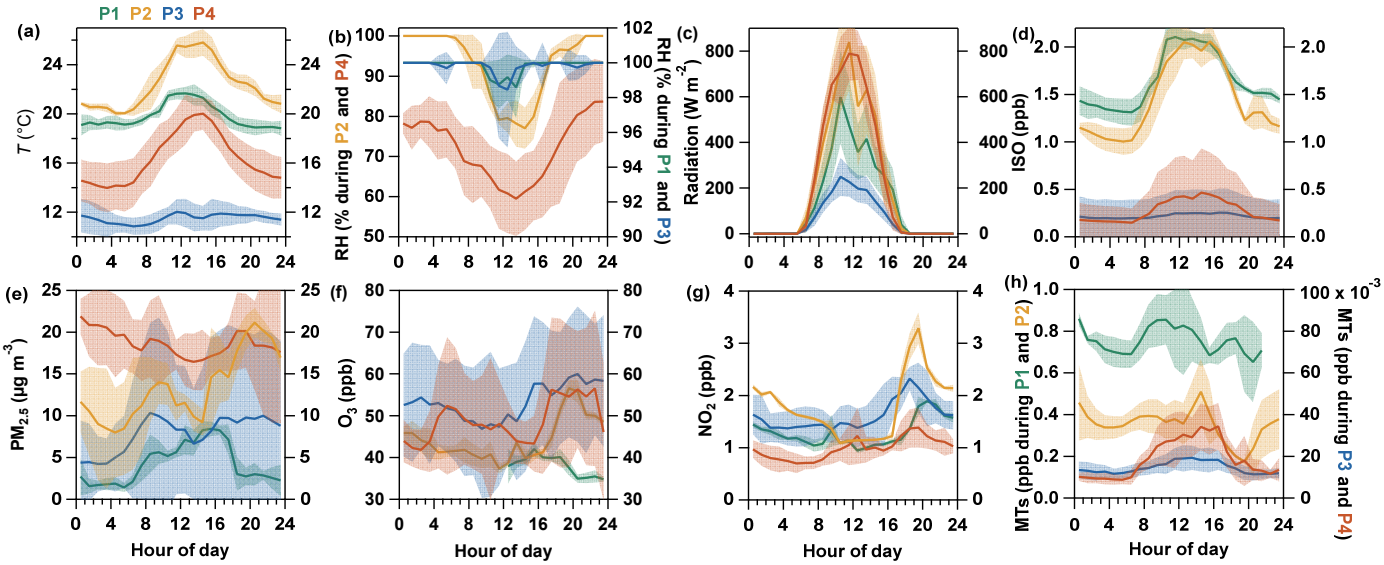


**Figure 1: Diurnal variations of (a-c) meteorological parameters, (e) $PM_{2.5}$ concentrations, (f-g) trace gases, (d, h) isoprene and monoterpenes during the selected four periods. The shaded areas indicate one standard deviation (±1σ) around the mean values.**

### 3.2 Overview of detected species by I-CIMS

A total of 1503 iodide-adduct ions were identified during the campaign. Based on elemental composition, these compounds were classified into five categories as shown in Fig. S3. Among them, CHO compounds, consisting solely of C, H, and O atoms, exhibited the largest contributions in both number and mixing ratio, with 701 species accounting for nearly half of the total mixing ratio. The second largest group was CHON compounds, containing C, H, O, and N atoms, comprising 583 species and contributing 29% of the total mixing ratio. As shown in the mass spectrum (Fig. 2a), CHO-OOMs exhibited a broad *m/z* distribution ranging from 170 to 480 Th. These compounds were mainly composed of organic acids, including small molecular carboxylic acids such as formic acid, acetic acid, glycolic acid, and lactic acid, as well as oxidation products derived from isoprene and terpenes, such as $C_4H_6O_3$, $C_5H_{10}O_3$, and $C_5H_8O_3$. In comparison, CHON-OOMs showed a relatively narrower *m/z* distribution, mainly concentrated between 180 and 380 Th. Major CHON species included amides (e.g., acetamide and hydroxyacetamide), nitrophenols (e.g., nitrophenol and methyl-nitrophenol), and ONs derived from isoprene and monoterpene oxidation (e.g., $C_{10}H_{15}NO_5$ and $C_{10}H_{15}NO_6$).

Figure 2b illustrates the variation in average carbon oxidation state ($OS_c$) as a function of carbon number for the two OOM classes. Overall, the average $OS_c$ increased with decreasing carbon number for both CHO- and CHON-OOMs, indicating that functionalization and fragmentation reactions dominated the aging processes of OOMs (Hunter et al., 2017; Kroll et al., 2011). However, CHON compounds with two carbon atoms exhibited significantly lower $OS_c$ values. This anomaly was mainly attributed to the high abundances of small amide compounds such as acetamide and hydroxyacetamide. At the relatively remote SH site, these compounds are likely influenced by regional transport associated with industrial emissions, a feature that is highly consistent with observations reported in 2022 (Zhang et al., 2024).

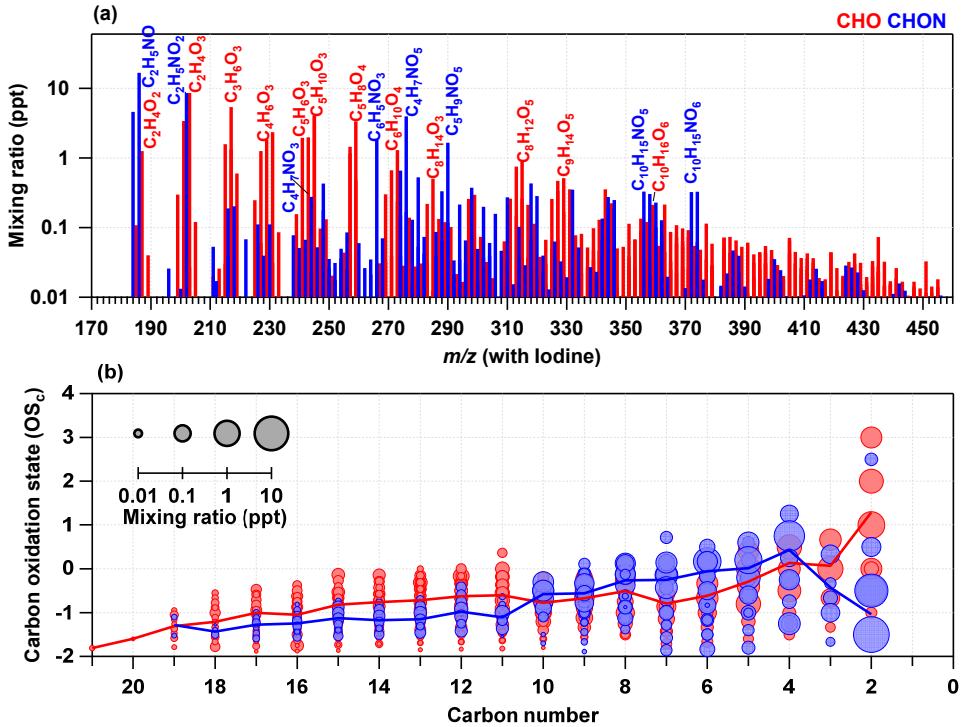


**Figure 2: (a) The average spectra of CHO and CHON molecules measured during the observation period. (b) The average carbon oxidation state of CHO and CHON molecules varies with different carbon numbers. The circle size corresponds to the mixing ratio of the molecules.**

Figure 3 presents the volatility distributions of CHO- and CHON-OOMs under different meteorological conditions. Overall, both classes were dominated by IVOCs, which accounted for 88% and 72% of CHO- and CHON-OOMs, respectively. In contrast, the contribution of LVOCs was less than 4% for both classes. Notably, under all meteorological conditions, the fraction of SVOCs in CHON-OOMs was consistently higher than that in CHO-OOMs, indicating that nitrogen-containing functional groups reduced molecular volatility. This result is consistent with previous observations conducted in Beijing during the winter of 2022 and summer of 2023 (Li et al., 2026). Previous studies have demonstrated that the addition of nitrogen-containing functional groups, particularly nitro and nitrate ester groups, can substantially decrease the saturation vapor pressure of organic molecules. Specifically, the introduction of one nitro group can reduce the saturation vapor pressure by approximately 0.34 orders of magnitude, while nitrate ester functionalities likewise contribute to lowering molecular volatility and enhancing condensability (Wu et al., 2021; Graham et al., 2023). These findings suggest that CHON-OOMs exhibit a stronger tendency to partition into the particle phase during gas–particle partitioning processes. Consistent with this finding, ONs have been shown to exhibit low volatility and readily partition into the particle phase at $NO_x$ concentrations below 6 ppb (Aruffo et al., 2022).

Furthermore, comparisons among different meteorological conditions revealed clear differences in volatility distributions. During cloud-influenced periods (P1 and P3), the contribution of IVOCs increased substantially, especially for CHON-OOMs

(82% under cloudy conditions versus 68% under clear conditions). In contrast, the fraction of SVOCs increased by approximately 14% during cloud-free periods (P2 and P4). The enhanced contribution of IVOCs during cloudy periods is likely associated with both efficient wet scavenging of lower-volatility compounds and aqueous-phase processing within cloud droplets. Due to their stronger affinity for the condensed phase, SVOCs and LVOCs are more readily absorbed into cloud droplets and subsequently removed through aqueous-phase processing and wet deposition. At the same time, aqueous-phase oxidation and fragmentation can generate smaller and more volatile products that are released into the gas phase, leading to a relative enrichment of IVOCs. In contrast, under cloud-free conditions with stronger solar radiation and enhanced photochemical activity, continuous oxidation of VOC precursors can promote the formation of more oxygenated and lower-volatility products, thereby increasing the relative contribution of SVOCs. Lower-volatility organic nitrates have also been shown to preferentially partition into the particle phase, consistent with their enhanced condensability (Aruffo et al., 2022). Additionally, the absence of cloud scavenging under clear conditions facilitates the accumulation of condensable species in the atmosphere. These results demonstrate that cloud processing and photochemical oxidation exert contrasting effects on OOM volatility, jointly shaping the gas-phase chemical composition of OOMs under different meteorological conditions. It should be noted that cloud occurrence coincided with concurrent changes in temperature, solar radiation, precursor concentrations, and air-mass characteristics. Therefore, the observed differences between cloud-influenced and cloud-free periods cannot be attributed to cloud processing alone. Rather, the observed OOM composition likely reflects the combined effects of cloud-related processing, precursor availability, atmospheric oxidation conditions, and meteorological variability, with these factors potentially interacting throughout the cloud-influenced periods.

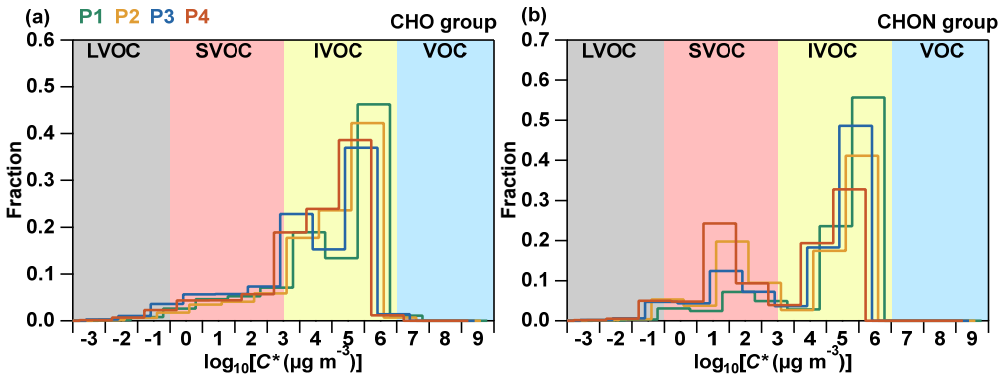


**Figure 3: The volatility distribution of (a) CHO and (b) CHON molecules under different meteorological conditions, where the volatility of gaseous organic molecules is represented by the saturated mass concentration ($C^*$) of organic molecules at 298 K. Volatility was estimated following the parameterization developed by Li et al. (2016). For clarity, the distributions are shown with vertical offsets.**

### 3.3 Diurnal pattern and oxidation pathways

#### 3.3.1 Non-nitrate biogenic oxidation products

Figure 4 illustrates the diurnal variations of non-nitrate oxidation products derived from biogenic isoprene and monoterpenes under different meteorological conditions. Previous studies have identified $C_4H_{6,8}O_{3,4}$ and $C_5H_{6,8,10}O_{3,4}$ as typical oxidation products of isoprene, whereas $C_{9,10}H_{14,16}O_{4,5}$ are commonly regarded as characteristic oxidation products of monoterpenes (Yu et al., 1999; Wennberg et al., 2018; Li et al., 2020). Distinct diurnal patterns were observed among the four periods. During the cloud-influenced period P1, nearly all oxidation products exhibited pronounced afternoon maxima. This pattern was likely driven by enhanced biogenic emissions under relatively high daytime temperature and solar radiation, which increased the availability of isoprene and monoterpenes (Fig. 1) and promoted their photochemical oxidation despite the presence of clouds. In addition, the high humidity and persistent cloud droplets during P1 may have facilitated aqueous-phase oxidation of water-soluble intermediates, contributing to the formation of oxygenated products through cloud processing (Altieri et al., 2006). Thus, although cloud-related uptake and removal occurred concurrently, the relatively strong precursor supply and oxidation conditions during P1 appear to have sustained net OOM production and the pronounced daytime enhancement.

In contrast, P3 was also strongly influenced by clouds and precipitation but occurred under substantially lower temperature and solar radiation. The resulting suppression of biogenic emissions (Hakola et al., 2006) reduced the availability of isoprene and monoterpenes and limited the formation of their oxidation products. Persistent precipitation and cloud processing may have further enhanced the removal of soluble OOMs and their precursors through aqueous-phase uptake and wet scavenging. Consequently, the much lower OOM concentrations in P3 likely resulted from the combined effects of reduced precursor emissions, weaker photochemical oxidation, and enhanced cloud- and precipitation-related removal. These contrasting responses indicate that the effects of clouds on OOM abundance cannot be considered independently of the meteorological conditions governing precursor emissions and atmospheric oxidation. During the warm and cloud-free period P2, the concentrations of these oxidation products gradually increased throughout the afternoon and reached their maxima around 20:00 local time, suggesting sustained production from daytime BVOC oxidation and subsequent accumulation under favourable meteorological conditions. Similar diurnal patterns have previously been reported in the Landes forest in France (Li et al., 2020). During the cloud-free but relatively cooler period P4, lower temperatures were less favourable for photochemical oxidation, leading to reduced concentrations of oxidation products and more subdued diurnal variations compared with P2. Overall, the results suggest that the abundance and diurnal evolution of biogenic non-nitrate OOMs are primarily governed by the interplay between biogenic precursor emissions atmospheric oxidation, and cloud-related processing. The contrasting responses during P1 and P3 indicate that the net influence of clouds depends strongly on meteorological conditions under which they occur, because enhanced aqueous-phase processing and removal can occur simultaneously with changes in radiation, temperature, and precursor availability.

To investigate the formation pathways of these non-nitrate biogenic oxidation products, the contributions of OH radicals and $O_3$ to their oxidation processes were evaluated using a kinetic approach (Text S3 and S5). Because the OH concentrations were

estimated rather than directly measured, the calculated rate ratios are best interpreted as relative reaction rates of the precursor VOCs with OH and $O_3$ under the observed conditions, rather than as quantitative contributions of the corresponding oxidation pathways to OOM production. The results indicate that isoprene oxidation was overwhelmingly dominated by OH radicals at both 20:00 and 09:00, with the reaction rate of isoprene + OH being approximately 15 times higher than that of isoprene + $O_3$. This finding is consistent with previous laboratory studies showing that the reaction rate constant of isoprene with OH radicals is several orders of magnitude larger than that with $O_3$ (Zhang et al., 2000; Khamaganov and Hites, 2001). In contrast, monoterpene oxidation exhibited a more complex oxidation regime. The estimated oxidation rate of monoterpenes by OH radicals was only about 1.5 times higher than that by $O_3$, suggesting that both oxidants contributed substantially to monoterpene processing. The observed diurnal variations in Fig. 4 provide additional qualitative evidence for these contrasting oxidation regimes. The pronounced daytime enhancement of both isoprene- and monoterpene-derived products is consistent with active photochemical oxidation, while the sustained abundance and delayed maxima of monoterpene-derived products, particularly during P2, suggest an additional contribution from ozonolysis. Taken together, the kinetic calculations and observed temporal patterns suggest that isoprene oxidation at the SH site was predominantly associated with OH chemistry, whereas monoterpene oxidation involved both daytime OH oxidation and $O_3$-initiated ozonolysis. The contrasting oxidation regimes of isoprene and monoterpenes likely contribute to the distinct molecular composition and temporal evolution of their oxidation products under different meteorological conditions.

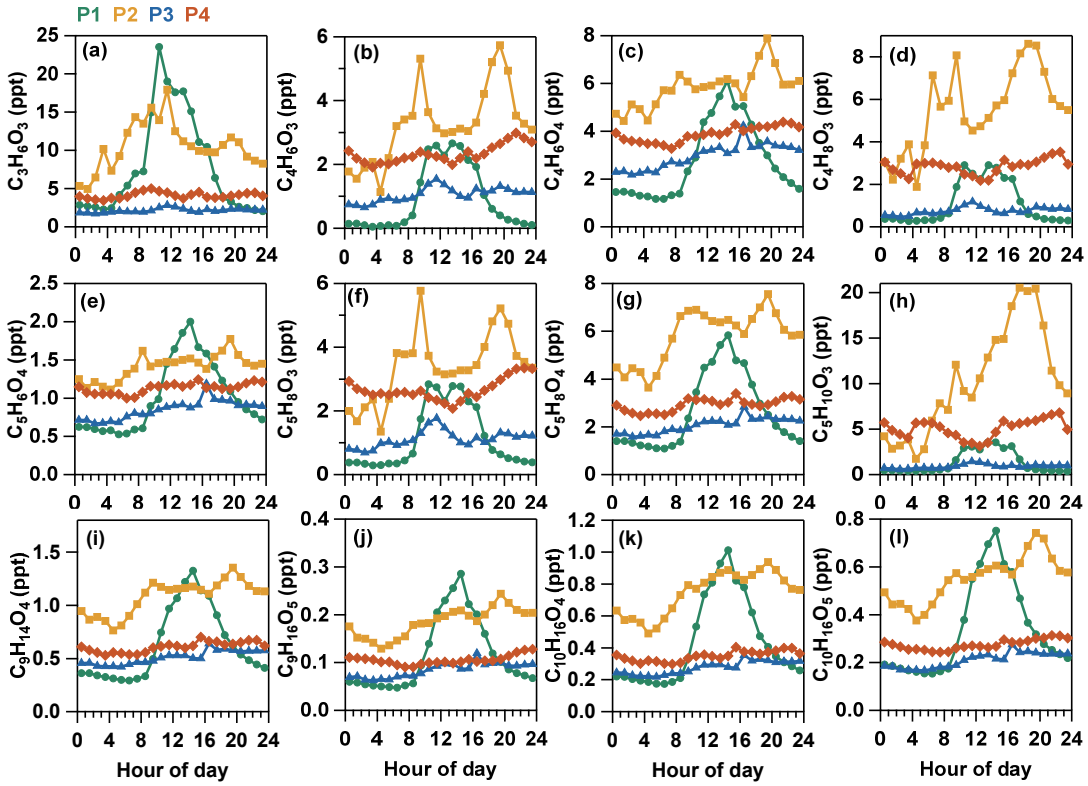

**Figure 4: Diurnal variations of (a-h) isoprene and (i-l) monoterpene non-nitrate oxidation products during four periods.**

### 3.3.2 Biogenic organic nitrates

ONs constituted an important class of gaseous OOMs at the SH site. During the observation period, a total of 47 ON species were identified, of which more than 80% were biogenic organic nitrates (Fig. S5). Figure 5 presents the diurnal variations of isoprene-derived organic nitrates (ISO-ONs) and monoterpene-derived organic nitrates (MT-ONs). As shown in the figure, except during P1, both species exhibited pronounced nocturnal maxima under all other meteorological conditions, with concentrations peaking at approximately 20:00 local time and decreasing substantially during daytime. Similar diurnal patterns have also been reported by Li et al. (2020) in the Landes forest in France, where biogenic ONs exhibited pronounced nighttime maxima associated with enhanced nocturnal oxidation chemistry. Kinetic calculations evaluating the relative contributions of $NO_3$-initiated oxidation pathways are provided in Text S4 and S6. The calculated oxidation rates indicate that O3 oxidation was more competitive than NO3 oxidation for isoprene, whereas $NO_3$ oxidation was more competitive than O3 oxidation for monoterpenes. These differences suggest potential contributions of these pathways to ON formation, but the rate calculations alone do not quantify their contributions to ON production. In contrast to the other ON species, $C_{10}H_{15,17}NO_6$ exhibited pronounced daytime peaks during P2, indicating that their formation may be associated with the reaction of organic peroxy radicals ($RO_2$) with NO, a pathway that becomes more important under daytime photochemical conditions. Similar formation mechanisms have been reported for multifunctional MT-ONs in environments influenced by both BVOC emissions and anthropogenic NOx (Lee et al., 2016). These multiple formation pathways reflect the complex coupling between BVOC oxidation and nitrogen oxide chemistry, highlighting the diverse sources and formation mechanisms of ONs in the atmosphere of high-altitude background sites.

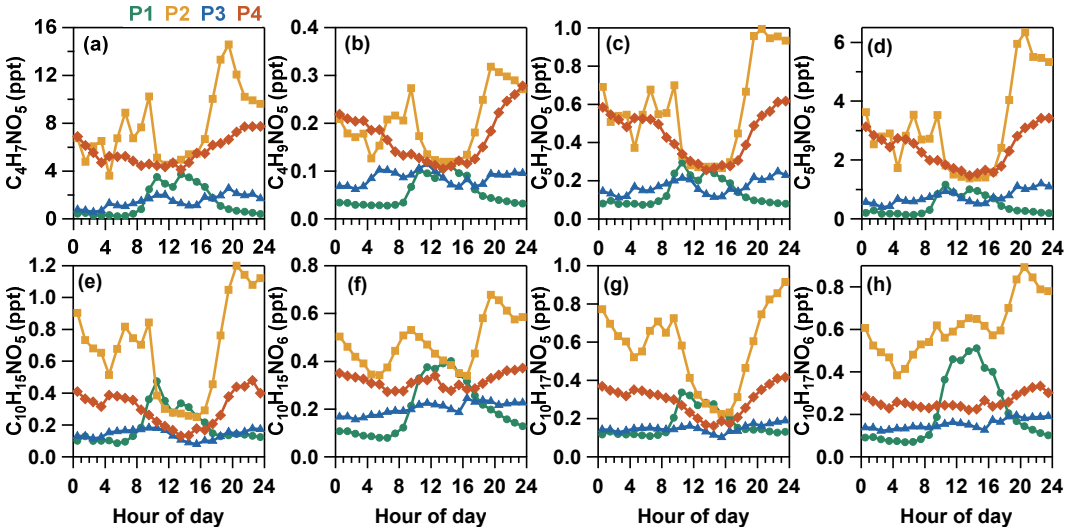


**Figure 5: Diurnal variation of (a-d) isoprene and (e-h) monoterpene organic nitrates among the four periods.**

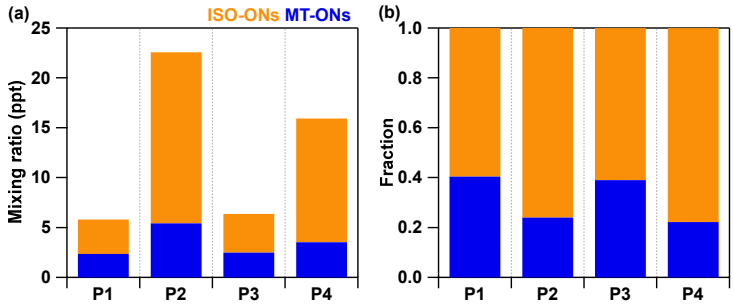


**Figure 6: (a) Mixing ratios and (b) relative contributions of isoprene-derived organic nitrates (ISO-ONs) and monoterpene-derived organic nitrates (MT-ONs) during the four periods.**

As shown in Fig. 6, the contributions of ISO-ONs and MT-ONs varied substantially under different meteorological conditions. During the cloud-influenced periods (P1 and P3), the concentrations of both ISO-ONs and MT-ONs decreased markedly due to efficient wet scavenging, with reductions of 75% and 46%, respectively, compared to cloud-free conditions. Although the decrease in ISO-ONs and MT-ONs during cloud periods is consistent with enhanced cloud-related removal, changes in precursor abundance and oxidation conditions may also contribute to the observed variability. Therefore, the observed changes in biogenic organic nitrates cannot be attributed to cloud processing alone and should be interpreted in the context of these concurrent atmospheric changes. To evaluate the influence of precursor variability, we additionally examined the ratios of ISO-ONs/isoprene and MT-ONs/monoterpenes (Fig. S6). The normalized ratios exhibited substantially different behaviours from the absolute concentrations, suggesting that precursor abundance alone cannot explain the observed variability in ONs. The elevated ONs/precursor ratios during P3 and P4 indicate that changes in oxidation conditions and ONs loss processes also played important roles. In addition to the overall decrease in concentration, their relative contributions also changed significantly during cloud events. The fraction of MT-ONs increased from 23% under cloud-free conditions to 40% during cloud-influenced periods, indicating distinct responses of ISO-ONs and MT-ONs to cloud processing. Several mechanisms may explain the enhanced contribution of MT-ONs during cloud events. First, the reaction rate of monoterpenes with $NO_3$ radicals is approximately one to two orders of magnitude higher than that of isoprene. Consequently, monoterpenes can be converted to MT-ONs more efficiently under conditions favourable for $NO_3$-initiated oxidation. This effect may be particularly important during cloud-influenced periods, when reduced solar radiation suppresses daytime OH oxidation and increases the relative importance of nighttime $NO_3$ chemistry. Second, differences in gas–particle partitioning and aqueous-phase processing may also contribute to the distinct responses of ISO-ONs and MT-ONs during cloud events. Differences in aqueous solubility among ONs may further affect their uptake into cloud droplets and subsequent removal. Previous modelling and observational studies have shown that isoprene-derived nitrates are generally more water-soluble and can contribute substantially to aqueous and in-cloud organic nitrate pools (Zare et al., 2019). Previous studies have demonstrated that certain ISO-ONs can be efficiently taken up by aqueous particles and undergo rapid hydrolysis in the condensed phase, whereas MT-ONs generally exhibit longer hydrolytic lifetimes (Vasquez et al., 2020; Wang et al., 2021). As a result, ISO-ONs may be more efficiently

removed through cloud uptake and subsequent aqueous-phase processing than MT-Ons, leading to an enrichment of MT-ONs in the remaining organic nitrate pool. These findings suggest that cloud processing not only reduces the overall abundance of biogenic ONs through wet scavenging but also alters their chemical composition by preferentially removing ISO-ONs relative to MT-ONs.

### 3.4 Source apportionment of OOMs

#### 3.4.1 Daytime OH-initiated BVOC oxidation

Among the nine PMF-resolved factors, two factors were associated with fresh daytime oxidation of BVOCs, namely Daytime ISO oxidation and Forenoon ISO+MT oxidation. Both factors were characterized by abundant low-carbon-number oxygenated products, including $C_3H_6O_3$, $C_4H_6O_3$, $C_4H_8O_3$, $C_5H_8O_3$, and $C_5H_8O_4$, which are widely recognized as first-generation oxidation products of isoprene (Wennberg et al., 2018). These compounds are typically formed through OH-initiated oxidation of BVOCs followed by reactions of $RO_2$ with $HO_2$ and NO, producing hydroxy carbonyls, hydroxy acids, and multifunctional oxygenated compounds (Berndt et al., 2019) . The Daytime ISO oxidation factor exhibited a pronounced midday maximum (Fig. 7c), consistent with peak solar radiation and enhanced daytime photochemical oxidation (Fig. 1). In contrast, the Forenoon ISO+MT oxidation factor peaked during the morning and contained both oxygenated products and organic nitrate species, including $C_4H_9NO_5$, $C_{10}H_{15}NO_5$, and $C_{10}H_{15}NO_6$ (Figs. 7a and S7). The coexistence of these compounds suggests a transition period during which residual nighttime oxidation products mixed with newly formed daytime oxidation products after sunrise. The strong correlation between these factors and ambient isoprene concentrations (r=0.75) further confirms the dominant role of biogenic emissions in driving their formation (Fig. S8). Non-parametric wind regression (NWR) analysis revealed that both factors were primarily associated with low wind speeds and local source regions (Fig. S9), indicating rapid formation from freshly emitted BVOCs. Together, these factors represent fresh daytime oxidation processes dominated by OH chemistry and local biogenic emissions. During P1 and P2, factors associated with daytime BVOC oxidation dominated the OOM budget (Fig. 8). In particular, the contribution of Daytime ISO oxidation increased substantially during the cloud-influenced P1 period, reaching its maximum around noon and accounting for approximately 39% of total OOMs. This observation suggests that despite enhanced wet scavenging, daytime oxidation of BVOCs remained an important source of gas-phase OOMs under cloud conditions, potentially facilitated by aqueous-phase photochemical processing and subsequent repartitioning of oxidation products to the gas phase.

#### 3.4.2 Aged photochemical oxidation and SOA precursor formation

Two additional PMF factors, Afternoon ISO oxidation and Afternoon ISO+MT oxidation, were characterized by pronounced afternoon maxima and a higher degree of oxidation (Fig. 7), indicating more advanced photochemical processing of BVOCs. The Afternoon ISO oxidation factor was distinguished by the presence of isoprene epoxydiols (IEPOX, $C_5H_{10}O_3$) and showed strong correlations with MVK+MACR (r=0.77, Fig. S8), two well-established oxidation products of isoprene. This factor also

contained $C_3H_6O_3$, $C_4H_8O_3$, $C_4H_7NO_5$, and $C_5H_9NO_4$. Bates et al. (2014) demonstrated that under low-NO conditions, ISOPOO radicals preferentially react with $HO_2$ to form ISOPOOH, which is subsequently oxidized to IEPOX. The relatively low afternoon NO concentrations observed at SH favour this pathway, resulting in enhanced production of IEPOX-related compounds. The delayed afternoon peak relative to the fresh oxidation factors reflects the multigenerational nature of this oxidation process. Notably, this factor showed a moderate correlation with the IEPOX-SOA factor resolved from ToF-ACSM measurements (r = 0.59), suggesting a link between gas-phase isoprene oxidation products and particle-phase IEPOX-SOA formation. This correlation may partly reflect gas-to-particle processing of isoprene oxidation products, but it may also arise from their common dependence on isoprene precursor abundance and photochemical activity. Therefore, the correlation should not be interpreted as direct evidence of a quantitative precursor–product relationship. Nevertheless, the concurrent variation of the Afternoon ISO oxidation factor and IEPOX-SOA is consistent with a role for gas–particle processing in the evolution of isoprene oxidation products and SOA formation at the SH site. The Afternoon ISO+MT oxidation factor was characterized by highly oxygenated products from both isoprene and monoterpenes, including $C_4H_6O_4$, $C_5H_6O_4$, $C_5H_8O_4$, $C_9H_{14}O_4$, $C_9H_{16}O_5$, and $C_{10}H_{16}O_5$. Compared with the fresh oxidation factors, NWR analysis indicated a greater influence of regional transport on the Afternoon ISO+MT oxidation factor. This result, combined with its highly oxygenated molecular composition, suggests that the factor represents relatively aged BVOC oxidation products that have undergone prolonged atmospheric processing before reaching the site. These aged photochemical factors were most pronounced during the warm and cloud-free P2 period (Fig. 8), when elevated temperatures and strong solar radiation favoured BVOC emissions and sustained photochemical processing. Together with Daytime ISO oxidation, they constituted the major fraction of OOMs during P2, consistent with the enhanced importance of secondary formation pathways under clear-sky conditions. Collectively, these two factors reflect the progression of BVOC oxidation from early-generation products to more oxidized species that contribute to SOA formation, providing evidence for the important role of photochemical aging in shaping the OOM composition at the SH site.

### 3.4.3 Nighttime BVOC oxidation

The Nighttime ISO+MT oxidation factor was dominated by ISO-ONs and MT-ONs and exhibited a pronounced nocturnal maximum at approximately 20:00 local time (Fig. 7). Characteristic compounds included a series of ISO-ONs and MT-ONs identified in Sect. 3.3.2, indicating that this factor represents nighttime oxidation chemistry involving reactive nitrogen species. The temporal behaviour of this factor closely followed the evening increases in $O_3$ and $NO_2$, which favour the formation of $NO_3$ radicals. As discussed previously, monoterpenes react rapidly with $NO_3$ radicals, while both $NO_3$-initiated oxidation and ozonolysis contribute to the formation of ONs. The pronounced nighttime peak therefore suggests that enhanced $NO_3$-initiated oxidation is an important chemical pathway contributing to this factor. NWR analysis showed that this factor was mainly associated with local source regions (Fig. S9), consistent with the short atmospheric lifetime of $NO_3$ radicals and the rapid formation of ONs near emission sources. Further evidence for the assignment of this factor to $NO_3$-initiated oxidation is provided by comparison with laboratory oxidation experiments (Zhang et al., 2026a). As shown in Fig. S10, after subtraction of the reagent ion, the characteristic mass spectrum of the Nighttime ISO+MT oxidation factor exhibits strong similarities to

the products generated from monoterpenes + $NO_3$ reactions in flowtube experiments, particularly within the *m/z* range of 200–300. Several major species, including $C_{10}H_{15}NO_5$, $C_{10}H_{17}NO_5$, $C_{10}H_{15}NO_6$, and $C_{10}H_{17}NO_6$, were observed in both spectra. These compounds are generally formed through the initial addition of $NO_3$ radicals to the double bonds of monoterpenes, followed by rapid $O_2$ addition and subsequent $RO_2$ radical reactions, yielding multifunctional ONs (Shen et al., 2021; Draper et al., 2019). The close agreement between the ambient PMF factor and laboratory-generated $NO_3$ oxidation products provides strong evidence that active nighttime oxidation of biogenic terpenes by $NO_3$ radicals occurred at the SH site and contributed substantially to the formation of nitrogen-containing OOMs. The importance of nighttime BVOC oxidation was particularly evident during the warm and cloud-free P2 period, when isoprene and monoterpene concentrations were comparable (Fig. S4). Under these conditions, daytime OOM production was dominated by isoprene oxidation, whereas the contribution of Nighttime ISO+MT oxidation increased substantially after sunset, highlighting the growing importance of nighttime monoterpene oxidation, particularly via $NO_3$ radicals. Gas–particle partitioning may also influence the temporal variation of condensable ONs. However, analysis of the TDLIF measurements showed that the particle-phase fraction of ONs, calculated as pONs/(pONs + gONs), did not increase during nighttime in P2. Instead, the ratio reached a maximum at approximately 16:00 and decreased after sunset (Fig. S11). This pattern suggests that the nocturnal enhancement of the Nighttime ISO+MT factor cannot be explained solely by increased partitioning to the particle phase and is more consistent with enhanced nighttime chemical production, particularly through $NO_3$-initiated oxidation.

Overall, the five biogenic PMF factors reveal a continuum of BVOC oxidation processes ranging from fresh daytime OH oxidation, through photochemical aging and SOA precursor formation, to nighttime $NO_3$-initiated oxidation. Their distinct temporal behaviours and source characteristics demonstrate the strong influence of oxidant availability, precursor emissions, and atmospheric processing on the formation and evolution of OOMs at the SH mountain site.

### 3.4.4 Anthropogenic and regional transport factors

In addition to the five BVOC-related factors discussed above, four PMF factors were attributed primarily to anthropogenic emissions and regional transport processes. Compared with the biogenic factors, these factors exhibited less pronounced diurnal variability and stronger transport signatures, highlighting the influence of anthropogenic activities on the molecular composition of OOMs at this high-altitude background site.

The first anthropogenic factor, termed Nitrogen-containing species, was characterized by abundant nitrophenols, ONs, and related nitrogen-containing compounds, including $C_6H_5NO_3$, $C_7H_7NO_3$, and $C_7H_{13}NO_5$. The factor exhibited a pronounced nighttime maximum and showed moderate correlations with aromatic hydrocarbons (Fig. S8). Nitrophenols are well-established tracers of anthropogenic influence and can originate from both primary emissions and secondary atmospheric processing (Harrison et al., 2005). Previous studies have identified biomass burning, residential combustion, and vehicle exhaust as important sources of nitrophenols, while secondary formation through the photooxidation and $NO_3$-initiated oxidation of aromatic hydrocarbons has also been widely reported (Wang et al., 2020; Wernis et al., 2022). The coexistence of nitrophenols and ONs within this factor therefore suggests mixed contributions from combustion-related emissions and

subsequent atmospheric oxidation processes. The NWR analysis further revealed clear transport characteristics, indicating that this factor was not solely associated with local emissions but was also influenced by regional transport of anthropogenic pollutants.

The Sulfur-containing species factor was characterized by organosulfur compounds, including $C_3H_8OS$, $C_9H_{10}OS$, and $C_9H_{10}O_8S$. Organosulfur species have attracted increasing attention because they can be formed through both primary emissions and secondary atmospheric processes. In particular, compounds such as $C_9H_{10}O_8S$ are likely related to organosulfate formation through multiphase reactions occurring in aerosol liquid water or cloud droplets (Li et al., 2024; Yang et al., 2025). The frequent cloud events observed at the SH site may provide favorable conditions for aqueous/multiphase processing and potentially enhance the formation of organosulfur compounds. A comparison of factor contributions before, during, and after cloud events revealed an increase in this factor during cloud events (Fig. 9), consistent with enhanced aqueous/multiphase processing (McNeill, 2015; Brüggemann et al., 2020). The positive relationship between sulfur-containing species and ambient humidity (Fig. S12) provides further evidence for the possible involvement of aqueous/multiphase processes. The summed concentration of sulfur-containing molecules increased with RH, indicating that their abundance was enhanced under more humid conditions. Elevated RH can increase aerosol liquid water content and promote cloud droplet formation, potentially facilitating the uptake and transformation of sulfur-containing precursors through multiphase reactions. However, precursor availability and changes in air-mass transport may also influence the abundance of sulfur-containing species, and these effects cannot be fully separated from those of cloud and humidity in the present observations. Therefore, the observed enhancement during cloud events and its positive relationship with RH are consistent with an important contribution from aqueous/multiphase processing, rather than providing evidence for a unique formation pathway.

The Anthropogenic organic nitrates factor was characterized by $C_4H_7NO_5$, $C_5H_9NO_5$, $C_7H_{13}NO_5$, and $C_9H_{15}NO_5$. Unlike the biogenic organic nitrate factor discussed in Section 3.4.3, this factor exhibited relatively weak diurnal variation, indicating a more aged and regionally mixed source. The factor showed strong correlations with more oxidized OOA (MO-OOA, r = 0.67) and particulate nitrate (r = 0.63), suggesting that it was associated with highly oxidized air masses and secondary aerosol formation. Previous studies have shown that anthropogenic ONs can be produced through the oxidation of anthropogenic VOCs under elevated $NO_x$ conditions and subsequently partition into regional aged aerosol (Lee et al., 2019; Zhu et al., 2025). The close relationship between this factor and MO-OOA therefore implies that both species may share similar source regions and atmospheric aging histories. Consistent with this interpretation, NWR analysis revealed a clear transport signal from the northwest, indicating that regional transport played a major role in controlling the abundance of this factor. The final factor, Regional transport, was characterized by $C_6H_4N_2$, $C_6H_5NO_3$, and $C_8H_{11}NO_2$. The presence of nitrogen-containing aromatic compounds, together with its strong correlation with MO-OOA (r = 0.62) and weak diurnal variability, suggests an association with aged anthropogenic air masses transported to the site. The similarity between the source characteristics of this factor and those of the Anthropogenic organic nitrates factor suggests that both originated from transported anthropogenic air masses that had undergone extensive atmospheric processing before arriving at the site. In contrast to P1 and P2, the relative contribution

of anthropogenic-related OOM factors increased markedly during P3 and P4, accounting for approximately 63% of total OOMs (Fig. 8). The decrease in temperature and BVOC precursor concentrations reduced the importance of biogenic oxidation pathways, whereas the contributions from sulfur-containing species, anthropogenic organic nitrates, and regional transport became increasingly prominent. This finding highlights the importance of regional transport of anthropogenic pollutants in shaping the chemical composition of OOMs and secondary organic aerosol at high-altitude background sites.

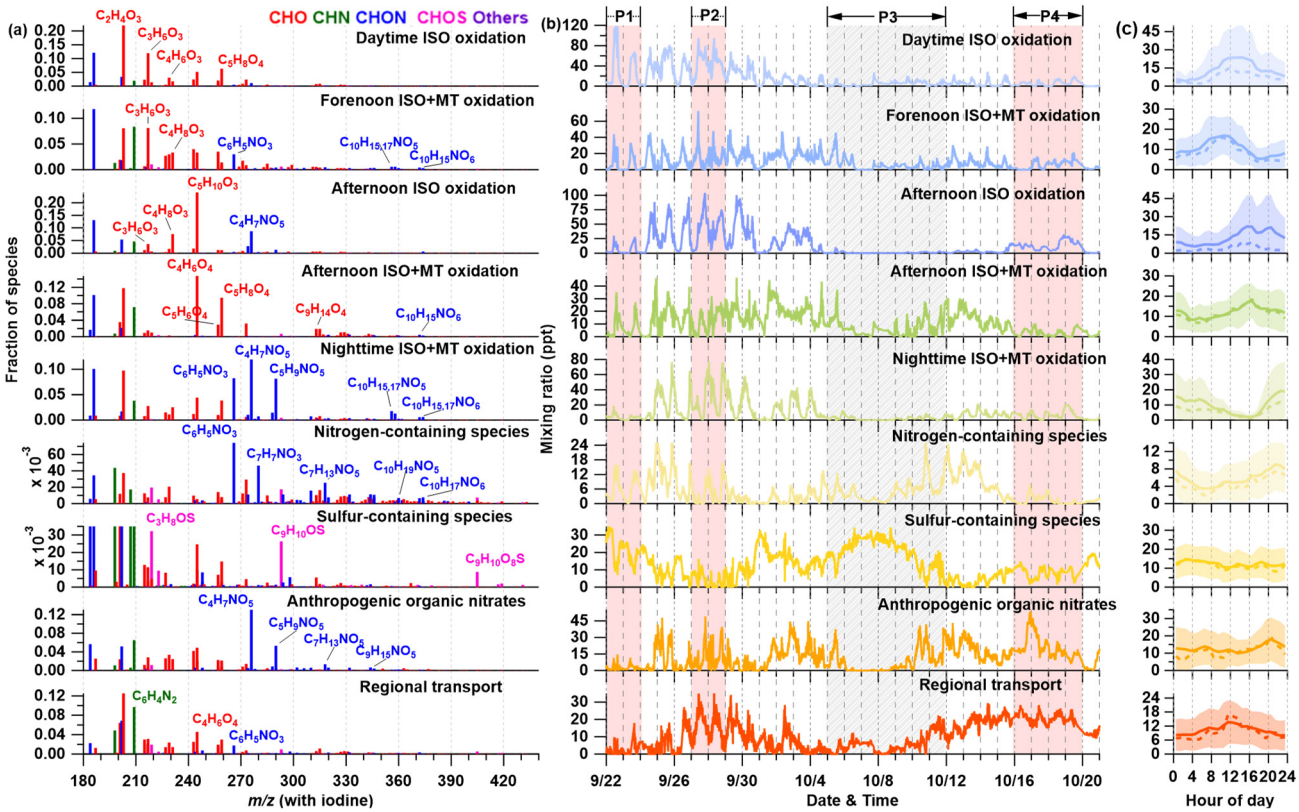


**Figure 7: (a) Mass spectra of the nine resolved OOMs factors. (b) Temporal variations and (c) diurnal patterns of the PMF-resolved OOM factors. For the diurnal patterns shown in panel (c), solid lines and dashed lines denote the mean and median values, respectively; and the shaded areas represent ±1 standard deviation around the mean.**

Overall, the factor contributions reveal a pronounced meteorological control on OOM sources and formation pathways. Warm conditions favoured local BVOC oxidation and the production of biogenic OOMs, whereas lower temperatures and changes in air-mass origin enhanced the influence of anthropogenic emissions and regional transport. Cloud events not only reduced OOM concentrations through wet scavenging but were also associated with changes in OOM chemical composition, including an enhanced contribution of sulfur-containing compounds consistent with a role for aqueous/multiphase processing. It should be noted that the oxidation pathways represented by the PMF factors are not necessarily mutually exclusive, as individual OOMs may be formed through multiple oxidation mechanisms. Thus, the PMF factors represent dominant chemical signatures

rather than uniquely resolved oxidation pathways, and some overlap among pathways is expected. These results demonstrate that the molecular composition of OOMs at the SH mountain site is jointly regulated by biogenic emissions, anthropogenic influences, and cloud-driven multiphase processing.

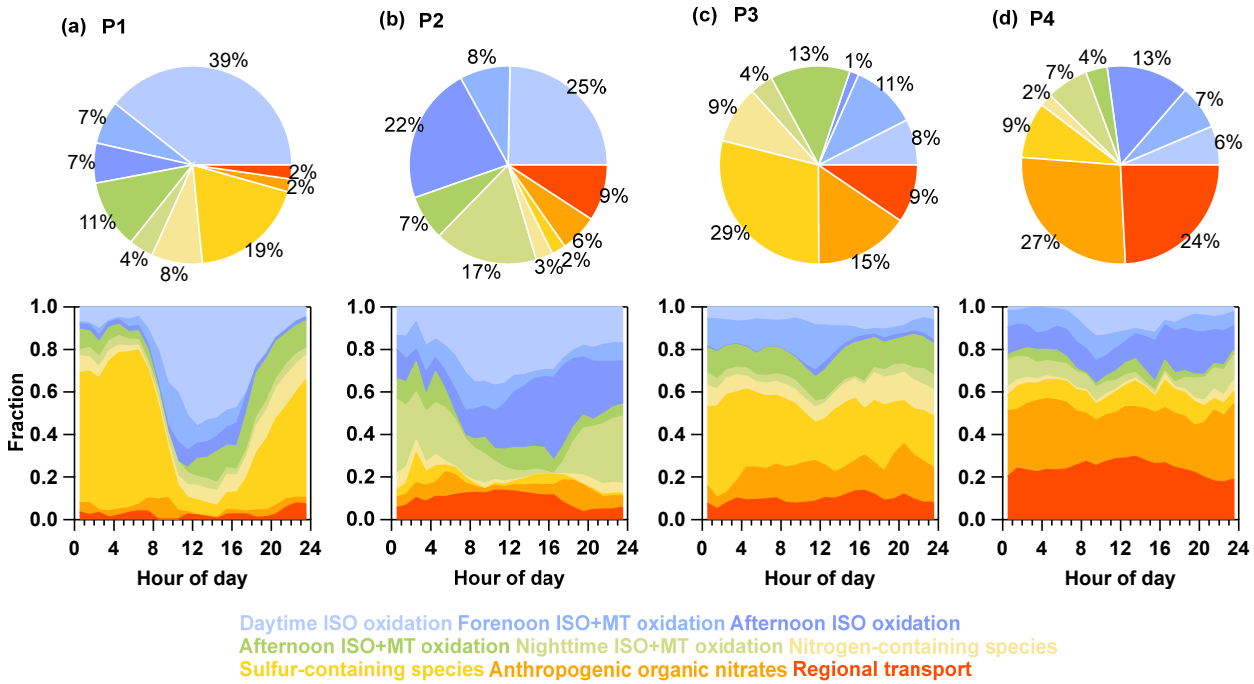


**Figure 8: Average contributions and diurnal variations of the PMF-resolved OOM factors during the four periods.**

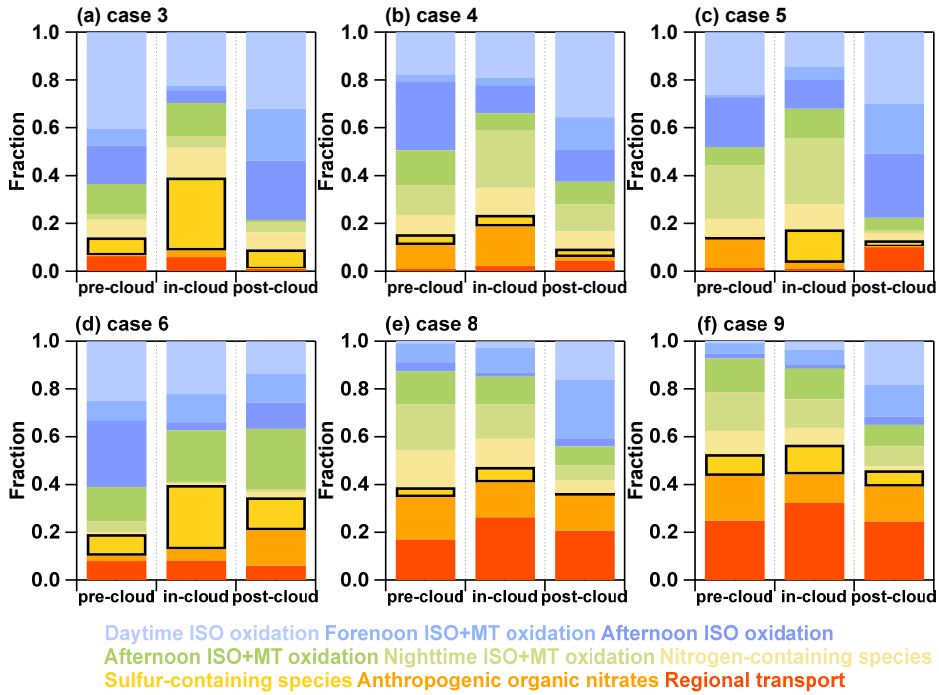


**Figure 9: Variations in the contributions of PMF-resolved OOM factors during the pre-cloud, in-cloud, and post-cloud stages.**

## 4 Conclusions

In this study, gas-phase oxygenated organic molecules (OOMs) were comprehensively characterized at a forested mountain station in southeastern China using an iodide-adduct chemical ionization time-of-flight mass spectrometer (I-CIMS). A total of 1503 iodide-adduct ions were identified, with CHO and CHON compounds constituting the dominant fraction of detected OOMs. Volatility analysis showed that intermediate-volatility organic compounds dominated both classes, while CHON compounds exhibited lower volatility than CHO compounds, indicating a stronger tendency for gas-to-particle partitioning. Distinct diurnal patterns of biogenic oxidation products were observed under different meteorological conditions. Kinetic analyses suggested that OH oxidation dominated the atmospheric processing of isoprene, whereas both $NO_3$ and OH oxidation pathways contributed substantially to monoterpene oxidation, resulting in contrasting formation mechanisms for non-nitrate and nitrate-containing biogenic OOMs.

Positive matrix factorization resolved nine physically meaningful OOM factors, including five biogenic oxidation factors and four anthropogenic-related factors. Biogenic oxidation was the dominant source of OOMs during warm periods, contributing 68–79% of total OOM abundance, whereas anthropogenic influences became increasingly important during cooler and more polluted conditions. The resolved factors revealed clear temporal segregation among daytime photochemical oxidation, afternoon-aged oxidation, and nighttime $NO_3$-radical-driven chemistry. Correlation analyses and wind-regression results

further indicated that most biogenic factors were primarily associated with local formation, while aged anthropogenic OOMs exhibited stronger signatures of regional transport.

Cloud processes exerted a substantial influence on OOM abundance and composition through wet scavenging and multiphase chemical processing. During cloud periods, concentrations of isoprene-derived and monoterpene-derived organic nitrates decreased by 75% and 46%, respectively, while the relative contribution of monoterpene organic nitrates increased from 23% to 40%, suggesting different responses of ISO-ONs and MT-ONs to cloud processing. At the same time, the enhanced contribution of sulfur-containing OOMs during cloud events, together with their positive relationship with ambient RH, was consistent with a contribution from aqueous/multiphase processing to organosulfur formation. Overall, these findings indicate that cloud processing can not only remove OOMs from the atmosphere but also alter their molecular composition and source contributions, emphasizing the coupled roles of BVOC emissions, anthropogenic pollutants, and multiphase chemistry in shaping the evolution of atmospheric organic matter in forested mountain environments.

**Data availability**

The data are available upon request from the corresponding author Yele Sun (sunyele@mail.iap.ac.cn).

**Author contributions**

YS designed the research. YiZ, YuZ, WX, WZ, YL, ZZ, BS, NZ, JW, EA and PDC conducted the measurements. YiZ, ZZ, YL, and YuZ analysed the data. LL, XP, EA and ZW reviewed and commented on the paper. YiZ, WZ and YS wrote the paper.

**Competing interests**

The contact author has declared that none of the authors has any competing interests.

**Acknowledgements**

The authors would like to thank Prof. Mikael Ehn and Prof. Siegfried Schobesberger for generously sharing their knowledge and experience regarding I-CIMS data analysis.

**Disclaimer**

Publisher's note: Copernicus Publications remains neutral with regard to jurisdictional claims made in the text, published maps, institutional affiliations, or any other geographical representation in this paper. The authors bear the ultimate responsibility for

providing appropriate place names. Views expressed in the text are those of the authors and do not necessarily reflect the views of the publisher.

**Financial support**

This work was supported by the National Natural Science Foundation of China (Nos. 42330605, 42377101, and 42575127).

**References**

Altieri, K. E., Carlton, A. G., Lim, H.-J., Turpin, B. J., and Seitzinger, S. P.: Evidence for Oligomer Formation in Clouds: Reactions of Isoprene Oxidation Products, Environ. Sci. Technol., 40, 4956-4960, 10.1021/es052170n, 2006.

Aruffo, E., Wang, J., Ye, J., Ohno, P., Qin, Y., Stewart, M., McKinney, K., Di Carlo, P., and Martin, S. T.: Partitioning of Organonitrates in the Production of Secondary Organic Aerosols from α-Pinene Photo-Oxidation, Environ. Sci. Technol., 56, 5421-5429, 10.1021/acs.est.1c08380, 2022.

Bates, K. H., Crounse, J. D., St. Clair, J. M., Bennett, N. B., Nguyen, T. B., Seinfeld, J. H., Stoltz, B. M., and Wennberg, P. O.: Gas phase production and loss of isoprene epoxydiols, J. Phys. Chem. A, 118, 1237-1246, 10.1021/jp4107958, 2014.

Berndt, T., Hyttinen, N., Herrmann, H., and Hansel, A.: First oxidation products from the reaction of hydroxyl radicals with isoprene for pristine environmental conditions, Commun. Chem., 2, 21, 10.1038/s42004-019-0120-9, 2019.

Bianchi, F., Kurtén, T., Riva, M., Mohr, C., Rissanen, M. P., Roldin, P., Berndt, T., Crounse, J. D., Wennberg, P. O., Mentel, T. F., Wildt, J., Junninen, H., Jokinen, T., Kulmala, M., Worsnop, D. R., Thornton, J. A., Donahue, N., Kjaergaard, H. G., and Ehn, M.: Highly Oxygenated Organic Molecules (HOM) from Gas-Phase Autoxidation Involving Peroxy Radicals: A Key Contributor to Atmospheric Aerosol, Chem. Rev., 119, 3472-3509, 10.1021/acs.chemrev.8b00395, 2019.

Brüggemann, M., Xu, R., Tilgner, A., Kwong, K. C., Mutzel, A., Poon, H. Y., Otto, T., Schaefer, T., Poulain, L., Chan, M. N., and Herrmann, H.: Organosulfates in Ambient Aerosol: State of Knowledge and Future Research Directions on Formation, Abundance, Fate, and Importance, Environ. Sci. Technol., 54, 3767-3782, 10.1021/acs.est.9b06751, 2020.

Di Carlo, P., Aruffo, E., Busilacchio, M., Giammaria, F., Dari-Salisburgo, C., Biancofiore, F., Visconti, G., Lee, J., Moller, S., Reeves, C. E., Bauguitte, S., Forster, G., Jones, R. L., and Ouyang, B.: Aircraft based four-channel thermal dissociation laser induced fluorescence instrument for simultaneous measurements of NO2, total peroxy nitrate, total alkyl nitrate, and HNO, Atmos. Meas. Tech., 6, 971-980, 10.5194/amt-6-971-2013, 2013.

Ding, S., Liu, D., Zhao, S., Wu, Y., Li, S., Pan, B., Teng, X., Li, W., Xu, W., Zhang, Y., Sun, Y., Wu, Y., Pan, X., Peng, X., Zhang, G., Bi, X., Tian, P., Liu, L., and Wang, Z.: Field Observation of Important Nonactivation Scavenging of Black Carbon by Clouds, Environ. Sci. Technol., 10.1021/acs.est.5c00199, 2025.

Draper, D. C., Myllys, N., Hyttinen, N., Møller, K. H., Kjaergaard, H. G., Fry, J. L., Smith, J. N., and Kurtén, T.: Formation of Highly Oxidized Molecules from NO3 Radical Initiated Oxidation of Δ-3-Carene: A Mechanistic Study, ACS Earth Space Chem., 3, 1460-1470, 10.1021/acsearthspacechem.9b00143, 2019.

Ehn, M., Thornton, J. A., Kleist, E., Sipila, M., Junninen, H., Pullinen, I., Springer, M., Rubach, F., Tillmann, R., Lee, B., Lopez-Hilfiker, F., Andres, S., Acir, I. H., Rissanen, M., Jokinen, T., Schobesberger, S., Kangasluoma, J., Kontkanen, J., Nieminen, T., Kurten, T., Nielsen, L. B., Jorgensen, S., Kjaergaard, H. G., Canagaratna, M., Maso, M. D., Berndt, T., Petaja, T., Wahner, A., Kerminen, V. M., Kulmala, M., Worsnop, D. R., Wildt, J., and Mentel, T. F.: A large source of low-volatility secondary organic aerosol, Nature, 506, 476-479, 10.1038/nature13032, 2014.

Ervens, B., Turpin, B. J., and Weber, R. J.: Secondary organic aerosol formation in cloud droplets and aqueous particles (aqSOA): a review of laboratory, field and model studies, Atmos. Chem. Phys., 11, 11069-11102, 10.5194/acp-11-11069-2011, 2011.

Graham, E., Wu, C., Bell, David M., Bertrand, A., Haslett, S., Baltensperger, U., Haddad, I., Krejci, R., Riipinen, I., and Mohr, C.: Volatility of aerosol particles from NO3 oxidation of various biogenic organic precursors, Atmos. Chem. Phys., 23, 7347-7362, 10.5194/acp-23-7347-2023, 2023.

Guenther, A., Hewitt, C. N., Erickson, D., Fall, R., Geron, C., Graedel, T., Harley, P., Klinger, L., Lerdau, M., McKay, W. A., Pierce, T., Scholes, B., Steinbrecher, R., Tallamraju, R., Taylor, J., and Zimmerman, P.: A global model of natural volatile organic compound emissions, J. Geophys. Res., 100, 10.1029/94jd02950, 1995.

Hakola, H., Tarvainen, V., Bäck, J., Ranta, H., Bonn, B., Rinne, J., and Kulmala, M.: Seasonal variation of mono- and sesquiterpene emission rates of Scots pine, Biogeosciences, 3, 93-101, 10.5194/bg-3-93-2006, 2006.

Hallquist, M., Wenger, J. C., Baltensperger, U., Rudich, Y., Simpson, D., Claeys, M., Dommen, J., Donahue, N. M., George, C., Goldstein, A. H., Hamilton, J. F., Herrmann, H., Hoffmann, T., Iinuma, Y., Jang, M., Jenkin, M. E., Jimenez, J. L., Kiendler-Scharr, A., Maenhaut, W., McFiggans, G., Mentel, T. F., Monod, A., Prévôt, A. S. H., Seinfeld, J. H., Surratt, J. D., Szmigielski, R., and Wildt, J.: The formation, properties and impact of secondary organic aerosol: current and emerging issues, Atmos. Chem. Phys., 9, 5155-5236, 10.5194/acp-9-5155-2009, 2009.

Harrison, M. A. J., Barra, S., Borghesi, D., Vione, D., Arsene, C., and Iulian Olariu, R.: Nitrated phenols in the atmosphere: a review, Atmos. Environ., 39, 231-248, 10.1016/j.atmosenv.2004.09.044, 2005.

Herrmann, H., Schaefer, T., Tilgner, A., Styler, S. A., Weller, C., Teich, M., and Otto, T.: Tropospheric Aqueous-Phase Chemistry: Kinetics, Mechanisms, and Its Coupling to a Changing Gas Phase, Chem. Rev., 115, 4259-4334, 10.1021/cr500447k, 2015.

Hersbach, H., Bell, B., Berrisford, P., Biavati, G., Horányi, A., Muñoz Sabater, J., Nicolas, J., Peubey, C., Radu, R., Rozum, I., Schepers, D., Simmons, A., Soci, C., Dee, D., and Thépaut, J.-N.: ERA5 hourly data on single levels from 1940 to present, Copernicus Climate Change Service (C3S) Climate Data Store (CDS), 10.24381/cds.adbb2d47, 2023.

Hoyle, C. R., Myhre, G., Berntsen, T. K., and Isaksen, I. S. A.: Anthropogenic influence on SOA and the resulting radiative forcing, Atmos. Chem. Phys., 9, 2715-2728, 10.5194/acp-9-2715-2009, 2009.

Hunter, J. F., Day, D. A., Palm, B. B., Yatavelli, R., Chan, A., Kaser, L., Cappellin, L., Hayes, P. L., Cross, E. S., and Carrasquillo, A. J. J. N. G.: Comprehensive characterization of atmospheric organic carbon at a forested site, Nat. Geosci., 10, 748-753, 2017.

Isaacman-VanWertz, G., Massoli, P., O'Brien, R., Lim, C., Franklin, J. P., Moss, J. A., Hunter, J. F., Nowak, J. B., Canagaratna, M. R., Misztal, P. K., Arata, C., Roscioli, J. R., Herndon, S. T., Onasch, T. B., Lambe, A. T., Jayne, J. T., Su, L., Knopf, D. A., Goldstein, A. H., Worsnop, D. R., and Kroll, J. H.: Chemical evolution of atmospheric organic carbon over multiple generations of oxidation, Nat. Chem., 10, 462-468, 10.1038/s41557-018-0002-2, 2018.

Junninen, H., Ehn, M., Petäjä, T., Luosujärvi, L., Kotiaho, T., Kostiainen, R., Rohner, U., Gonin, M., Fuhrer, K., Kulmala, M., and Worsnop, D. R.: A high-resolution mass spectrometer to measure atmospheric ion composition, Atmos. Meas. Tech., 3, 1039-1053, 10.5194/amt-3-1039-2010, 2010.

Khamaganov, V. G. and Hites, R. A.: Rate Constants for the Gas-Phase Reactions of Ozone with Isoprene, α- and β-Pinene, and Limonene as a Function of Temperature, J. Phys. Chem. A, 105, 815-822, 10.1021/jp002730z, 2001.

Kroll, J. H., Donahue, N. M., Jimenez, J. L., Kessler, S. H., Canagaratna, M. R., Wilson, K. R., Altieri, K. E., Mazzoleni, L. R., Wozniak, A. S., Bluhm, H., Mysak, E. R., Smith, J. D., Kolb, C. E., and Worsnop, D. R.: Carbon oxidation state as a metric for describing the chemistry of atmospheric organic aerosol, Nat. Chem., 3, 133-139, 10.1038/nchem.948, 2011.

Lee, A. K. Y., Adam, M. G., Liggio, J., Li, S. M., Li, K., Willis, M. D., Abbatt, J. P. D., Tokarek, T. W., Odame-Ankrah, C. A., Osthoff, H. D., Strawbridge, K., and Brook, J. R.: A large contribution of anthropogenic organo-nitrates to secondary organic aerosol in the Alberta oil sands, Atmos. Chem. Phys., 19, 12209-12219, 10.5194/acp-19-12209-2019, 2019.

Lee, B. H., Lopez-Hilfiker, F. D., Mohr, C., Kurtén, T., Worsnop, D. R., and Thornton, J. A.: An Iodide-Adduct High-Resolution Time-of-Flight Chemical-Ionization Mass Spectrometer: Application to Atmospheric Inorganic and Organic Compounds, Environ. Sci. Technol., 48, 6309-6317, 10.1021/es500362a, 2014.

Lee, B. H., Mohr, C., Lopez-Hilfiker, F. D., Lutz, A., Hallquist, M., Lee, L., Romer, P., Cohen, R. C., Iyer, S., Kurtén, T., Hu, W., Day, D. A., Campuzano-Jost, P., Jimenez, J. L., Xu, L., Ng, N. L., Guo, H., Weber, R. J., Wild, R. J., Brown, S. S., Koss, A., de Gouw, J., Olson, K., Goldstein, A. H., Seco, R., Kim, S., McAvey, K., Shepson, P. B., Starn, T., Baumann, K., Edgerton, E. S., Liu, J., Shilling, J. E., Miller, D. O., Brune, W., Schobesberger, S., D'Ambro, E. L., and Thornton, J. A.: Highly functionalized organic nitrates in the southeast United States: Contribution to secondary organic aerosol and reactive nitrogen budgets, Proc. Natl. Acad. Sci. U.S.A., 113, 1516-1521, 10.1073/pnas.1508108113, 2016.

Li, H., Riva, M., Rantala, P., Heikkinen, L., and Bianchi, F.: Terpenes and their oxidation products in the French Landes forest: insights from Vocus PTR-TOF measurements, Atmos. Chem. Phys., 20, 1941-1959, 10.5194/acp-20-1941-2020, 2020.

Li, L., Li, J., Zhang, X., Lin, Y., Wang, R., Cao, J., and Han, Y.: Effects of relative humidity on atmospheric organosulfur species derived from photooxidation and nocturnal chemistry in a forest environment, Environ. Pollut., 363, 125253, 10.1016/j.envpol.2024.125253, 2024.

Li, Y., Pöschl, U., and Shiraiwa, M.: Molecular corridors and parameterizations of volatility in the chemical evolution of organic aerosols, Atmos. Chem. Phys., 16, 3327-3344, 10.5194/acp-16-3327-2016, 2016.

Li, Y., Zhou, W., Sun, J., Lei, L., Xu, W., Zhang, Z., Zhang, Y., Du, A., Ye, P., Wang, J., Aruffo, E., Wang, Z., Worsnop, D. R., and Sun, Y.: Oxygenated organic molecules in urban Beijing: Contrasting summer–winter composition, sources, and roles in secondary organic aerosol formation, Environ. Sci. Technol., 60, 4990-5004, 10.1021/acs.est.5c17177, 2026.

Liu, Q., Shen, X., Sun, J., Zhang, Y., Qi, B., Ma, Q., Han, L., Xu, H., Hu, X., Lu, J., Liu, S., Yu, A., Liang, L., Gao, Q., Wang, H., Che, H., and Zhang, X.: Characterization of fog microphysics and their relationships with visibility at a mountain site in China, Atmos. Chem. Phys., 25, 3253-3267, 10.5194/acp-25-3253-2025, 2025.

McNeill, V. F.: Aqueous Organic Chemistry in the Atmosphere: Sources and Chemical Processing of Organic Aerosols, Environ. Sci. Technol., 49, 1237-1244, 10.1021/es5043707, 2015.

Mohr, C., Thornton, J. A., Heitto, A., Lopez-Hilfiker, F. D., Lutz, A., Riipinen, I., Hong, J., Donahue, N. M., Hallquist, M., Petäjä, T., Kulmala, M., and Yli-Juuti, T.: Molecular identification of organic vapors driving atmospheric nanoparticle growth, Nat. Commun., 10, 4442, 10.1038/s41467-019-12473-2, 2019.

Shen, H., Zhao, D., Pullinen, I., Kang, S., Vereecken, L., Fuchs, H., Acir, I.-H., Tillmann, R., Rohrer, F., Wildt, J., Kiendler-Scharr, A., Wahner, A., and Mentel, T. F.: Highly Oxygenated Organic Nitrates Formed from NO3 Radical-Initiated Oxidation of β-Pinene, Environ. Sci. Technol., 55, 15658-15671, 10.1021/acs.est.1c03978, 2021.

Shen, X., Liu, Q., Sun, J., Kong, W., Ma, Q., Qi, B., Han, L., Zhang, Y., Liang, L., Liu, L., Liu, S., Hu, X., Lu, J., Yu, A., Che, H., and Zhang, X.: Measurement report: The influence of particle number size distribution and hygroscopicity on the microphysical properties of cloud droplets at a mountain site, Atmos. Chem. Phys., 25, 5711-5725, 10.5194/acp-25-5711-2025, 2025.

Shingler, T., Dey, S., Sorooshian, A., Brechtel, F. J., Wang, Z., Metcalf, A., Coggon, M., Mülmenstädt, J., Russell, L. M., Jonsson, H. H., and Seinfeld, J. H.: Characterisation and airborne deployment of a new counterflow virtual impactor inlet, Atmos. Meas. Tech., 5, 1259-1269, 10.5194/amt-5-1259-2012, 2012.

Sun, J. and Ariya, P. A.: Atmospheric organic and bio-aerosols as cloud condensation nuclei (CCN): A review, Atmos. Environ., 40, 795-820, 10.1016/j.atmosenv.2005.05.052, 2006.

Sun, Y., Luo, H., Li, Y., Zhou, W., Xu, W., Fu, P., and Zhao, D.: Atmospheric organic aerosols: online molecular characterization and environmental impacts, npj Clim. Atmos. Sci., 8, 305, 10.1038/s41612-025-01199-2, 2025.

Takeuchi, M. and Ng, N. L.: Chemical composition and hydrolysis of organic nitrate aerosol formed from hydroxyl and nitrate radical oxidation of α-pinene and β-pinene, Atmos. Chem. Phys., 19, 12749-12766, 10.5194/acp-19-12749-2019, 2019.

Tröstl, J., Chuang, W. K., Gordon, H., Heinritzi, M., Yan, C., Molteni, U., Ahlm, L., Frege, C., Bianchi, F., Wagner, R., Simon, M., Lehtipalo, K., Williamson, C., Craven, J. S., Duplissy, J., Adamov, A., Almeida, J., Bernhammer, A.-K., Breitenlechner, M., Brilke, S., Dias, A., Ehrhart, S., Flagan, R. C., Franchin, A., Fuchs, C., Guida, R., Gysel, M., Hansel, A., Hoyle, C. R., Jokinen, T., Junninen, H., Kangasluoma, J., Keskinen, H., Kim, J., Krapf, M., Kürten, A., Laaksonen, A., Lawler, M., Leiminger, M., Mathot, S., Möhler, O., Nieminen, T., Onnela, A., Petäjä, T., Piel, F. M., Miettinen, P., Rissanen, M. P., Rondo, L., Sarnela, N., Schobesberger, S., Sengupta, K., Sipilä, M., Smith, J. N., Steiner, G., Tomè, A., Virtanen, A., Wagner, A. C., Weingartner, E., Wimmer, D., Winkler, P. M., Ye, P., Carslaw, K. S., Curtius, J., Dommen, J., Kirkby, J., Kulmala, M.,

Riipinen, I., Worsnop, D. R., Donahue, N. M., and Baltensperger, U.: The role of low-volatility organic compounds in initial particle growth in the atmosphere, Nature, 533, 527-531, 10.1038/nature18271, 2016.

Ulbrich, I. M., Canagaratna, M. R., Zhang, Q., Worsnop, D. R., and Jimenez, J. L.: Interpretation of organic components from Positive Matrix Factorization of aerosol mass spectrometric data, Atmos. Chem. Phys., 9, 2891-2918, 10.5194/acp-9-2891-2009, 2009.

Vasquez, K. T., Crounse, J. D., Schulze, B. C., Bates, K. H., Teng, A. P., Xu, L., Allen, H. M., and Wennberg, P. O.: Rapid hydrolysis of tertiary isoprene nitrate efficiently removes NOx from the atmosphere, Proc. Natl. Acad. Sci., 117, 33011-33016, 10.1073/pnas.2017442117, 2020.

Wang, H., Gao, Y., Wang, S., Wu, X., Liu, Y., Li, X., Huang, D., Lou, S., Wu, Z., Guo, S., Jing, S., Li, Y., Huang, C., Tyndall, G. S., Orlando, J. J., and Zhang, X.: Atmospheric Processing of Nitrophenols and Nitrocresols From Biomass Burning Emissions, J. Geophys. Res. Atmos., 125, e2020JD033401, 10.1029/2020JD033401, 2020.

Wang, Y., Piletic, I. R., Takeuchi, M., Xu, T., France, S., and Ng, N. L.: Synthesis and Hydrolysis of Atmospherically Relevant Monoterpene-Derived Organic Nitrates, Environ. Sci. Technol., 55, 14595-14606, 10.1021/acs.est.1c05310, 2021.

Wang, Z., Pan, X., Sun, Y., Xin, J., Su, H., Cao, J., Li, J., Yang, T., Liu, H., Yao, W., Xu, W., Chen, X., Zhou, W., Ma, Y., Cheng, X., Ye, J., Hu, B., Jiang, R., Wang, Z., Ge, B., Wu, L., Li, X., Li, J., Wu, Z., Kong, L., Zhu, M., Jia, J., Li, X., Fang, X., and Liu, L.: Atmospheric Boundary Layer Eco-Environment Shanghuang Observatory: An Integrated Multiscale Research Platform in Southeastern China for Understanding Boundary Layer Processes, Atmospheric Chemistry Feedback, and Extreme Weather–Climate Linkages, Adv. Atmos. Sci., 43, 1-9, 10.1007/s00376-025-5307-7, 2025.

Wennberg, P. O., Bates, K. H., Crounse, J. D., Dodson, L. G., McVay, R. C., Mertens, L. A., Nguyen, T. B., Praske, E., Schwantes, R. H., Smarte, M. D., St Clair, J. M., Teng, A. P., Zhang, X., and Seinfeld, J. H.: Gas-Phase Reactions of Isoprene and Its Major Oxidation Products, Chemical Reviews, 118, 3337-3390, 10.1021/acs.chemrev.7b00439, 2018.

Wernis, R. A., Kreisberg, N. M., Weber, R. J., Drozd, G. T., and Goldstein, A. H.: Source apportionment of VOCs, IVOCs and SVOCs by positive matrix factorization in suburban Livermore, California, Atmos. Chem. Phys., 22, 14987-15019, 10.5194/acp-22-14987-2022, 2022.

Wu, C., Bell, D. M., Graham, E. L., Haslett, S., Riipinen, I., Baltensperger, U., Bertrand, A., Giannoukos, S., Schoonbaert, J., El Haddad, I., Prevot, A. S. H., Huang, W., and Mohr, C.: Photolytically induced changes in composition and volatility of biogenic secondary organic aerosol from nitrate radical oxidation during night-to-day transition, Atmos. Chem. Phys., 21, 14907-14925, 10.5194/acp-21-14907-2021, 2021.

Yang, N., Wang, J., Jacob, D. J., Ye, J., Sheng, M., Niu, M., Qin, Y., Ge, X., Sun, Y., Wang, Z., Wang, Y., Wu, F., Liu, C.-Q., George, C., and Fu, P.: Aqueous production of sulfur-containing aerosols from nitroaromatic compounds and SO2 in wintertime urban haze, Sci. Bull., 70, 1846-1855, 10.1016/j.scib.2025.03.013, 2025.

Ye, C., Yuan, B., Lin, Y., Wang, Z., Hu, W., Li, T., Chen, W., Wu, C., Wang, C., Huang, S., Qi, J., Wang, B., Wang, C., Song, W., Wang, X., Zheng, E., Krechmer, J. E., Ye, P., Zhang, Z., Wang, X., Worsnop, D. R., and Shao, M.: Chemical

characterization of oxygenated organic compounds in the gas phase and particle phase using iodide CIMS with FIGAERO in urban air, Atmos. Chem. Phys., 21, 8455-8478, 10.5194/acp-21-8455-2021, 2021.

Yu, J., Griffin, R. J., Cocker, D. R., Flagan, R. C., Seinfeld, J. H., and Blanchard, P.: Observation of gaseous and particulate products of monoterpene oxidation in forest atmospheres, Geophys. Res. Lett., 26, 1145-1148, 10.1029/1999gl900169, 1999.

Yu, Y., Guo, S., Tan, R., Ni, X., Wan, Z., Ye, C., and Hu, M.: Evaluation of Anthropogenic Influences on Atmospheric Oxygenated Organic Molecules in Both Gas and Particle Phases over the Southeastern Tibetan Plateau, ACS ES&T Air, 2, 2175-2183, 10.1021/acsestair.5c00135, 2025.

Zare, A., Fahey, K. M., Sarwar, G., Cohen, R. C., and Pye, H. O. T.: Vapor-Pressure Pathways Initiate but Hydrolysis Products Dominate the Aerosol Estimated from Organic Nitrates, ACS Earth Space Chem., 3, 1426-1437, 10.1021/acsearthspacechem.9b00067, 2019.

Zha, Q., Aliaga, D., Krejci, R., Sinclair, V. A., Wu, C., Ciarelli, G., Scholz, W., Heikkinen, L., Partoll, E., Gramlich, Y., Huang, W., Leiminger, M., Enroth, J., Peräkylä, O., Cai, R., Chen, X., Koenig, A. M., Velarde, F., Moreno, I., Petäjä, T., Artaxo, P., Laj, P., Hansel, A., Carbone, S., Kulmala, M., Andrade, M., Worsnop, D., Mohr, C., and Bianchi, F.: Oxidized organic molecules in the tropical free troposphere over Amazonia, Natl. Sci. Rev., 11, nwad138, 10.1093/nsr/nwad138, 2024.

Zhang, J., Zhang, Y., Koskenvaara, H., Zhao, J., and Ehn, M.: Gas-phase products from nitrate radical oxidation of five monoterpenes: insights from free-jet flow-tube experiments, Atmos. Chem. Phys., 26, 3933-3949, 10.5194/acp-26-3933-2026, 2026a.

Zhang, R., Suh, I., Lei, W., Clinkenbeard, A. D., and North, S. W.: Kinetic studies of OH-initiated reactions of isoprene, J. Geophys. Res. Atmos., 105, 24627-24635, 10.1029/2000JD900330, 2000.

Zhang, Y., Xu, W., Zhou, W., Li, Y., Zhang, Z., Du, A., Qiao, H., Kuang, Y., Liu, L., Zhang, Z., He, X., Cheng, X., Pan, X., Fu, Q., Wang, Z., Ye, P., Worsnop, D. R., and Sun, Y.: Characterization of organic vapors by a Vocus proton-transfer-reaction mass spectrometry at a mountain site in southeastern China, Sci. Total Environ., 919, 170633, 10.1016/j.scitotenv.2024.170633, 2024.

Zhang, Y., Xu, W., Li, Y., Zhang, G., Liu, D., Kuang, Y., Zhang, Y., Zhou, W., Peng, X., Su, B., Huang, W., Zhang, Z., Yang, L., Wu, Y., Li, S., Zhao, S., Liu, L., Pan, X., Wang, Z., Bi, X., Ehn, M., Worsnop, D. R., and Sun, Y.: Seasonal variability and cloud-type effects on secondary organic aerosol formation during cloud events at a mountainous site in southeastern China, Atmos. Chem. Phys., 26, 5617-5634, 10.5194/acp-26-5617-2026, 2026b.

Zhang, Z., Yuan, Q., Wang, J., Jiang, J., Xu, W., Zeng, S., Zhang, Y., Zhou, W., Li, Y., Huang, X., Chen, X., Xia, M., Yan, C., Hu, B., Wang, Z., Li, J., Liu, Y., Kulmala, M., Worsnop, D. R., and Sun, Y.: Oxygenated Organic Molecules Drive Particle Growth and Secondary Organic Aerosol Formation in Beijing Winter, Environ. Sci. Technol. Lett., 13, 713-719, 10.1021/acs.estlett.6c00009, 2026c.

Zhu, W., Shi, J., Guo, S., Wang, Q., Chen, J., Lou, S., and Hu, M.: Comparative analysis of methods for seasonal particulate organic nitrate estimation in urban areas, npj Clim. Atmos. Sci., 8, 21, 10.1038/s41612-025-00904-5, 2025.